Effect of inhomogeneities on spiral wave dynamics in the Belousov-Zhabotinsky reaction

Linda B. Smolka*
Department of Mathematics, Duke University, Durham, North Carolina 27708, USA
and Department of Mathematics, Bucknell University, Lewisburg, Pennsylvania 17837, USA

Bradley Marts and Anna L. Lin†
Center for Nonlinear and Complex Systems and Department of Physics, Duke University, Durham, North Carolina 27708, USA
(Received 25 July 2005; published 8 November 2005)

We examine the effects of controlled, slowly varying spatial inhomogeneities on spiral wave dynamics in the light sensitive Belousov-Zhabotinsky chemical reaction-diffusion system. We measure the speed of the grain boundary that separates two spirals, the speed of the lower frequency spiral being swept away by the grain boundary, and the speed of the slow drift of the highest frequency spiral. The grain boundary speeds are shown to be related to the frequency of rotation and wave number of the spiral pattern, as predicted from analysis of the complex Ginzburg-Landau equation [M. Hendrey *et al.*, Phys. Rev. Lett. **82**, 859 (1999); M. Hendrey, *et al.*, Phys. Rev. E **61**, 4943 (2000)].

DOI: 10.1103/PhysRevE.72.056205 PACS number(s): 05.45.Xt, 82.40.Ck, 82.50.Hp, 82.50.Nd

I. INTRODUCTION

The formation of spirals is a widely observed phenomena in oscillatory and excitable systems with two-dimensional or quasi-two-dimensional spatial extent. Examples include cardiac tissue [1,2], slime mold colonies [3,4], chemical oscillators (such as the Belousov-Zhabotinsky (BZ) reaction) and surface reactions [5]. While several studies have focused on spiral dynamics in homogeneous conditions [6–11], more recent works have studied the effects of inhomogeneous conditions [2,8,12–20]; the condition more commonly found in nature. In particular, experimental studies under inhomogeneous conditions have examined spiral drift [8,21], a dispersion relation for a single spiral [12], the interaction between spiral and target patterns [17], and the role of coupling in an excitable medium (chick embryonic heart cells) on spiral formation [2].

Here we describe our experimental examination of the effect of slowly varying spatial inhomogeneities on the spiral wave dynamics in the BZ system. It is well known that the spiral frequency in the BZ reaction is light sensitive. Typically the frequency decreases as light intensity increases [10,12,22], although it has been shown for specific chemical conditions the opposite effect is attainable [10]. Using a similar experimental setup as [22], we use light to impose a spatial inhomogeneity in our experiments and measure aspects of the spiral dynamics under those inhomogeneous conditions.

An example of spiral traveling waves in the BZ reaction is shown in Fig. 1(i). Each spiral vortex (core) is a pacemaker that rotates, generating spiral excitation waves that travel radially outward so that away from the vortex each point in space oscillates in time. The core of a spiral sets the temporal frequency of the entire spiral domain associated with that particular core. When traveling waves of neighboring vortices collide they annihilate each other. This interaction of colliding wave fronts results in a defect in the spiral pattern (called the grain boundary) which separates neighboring spiral domains [6]. In nature, oscillatory phenomena often occur under conditions which are spatially heterogeneous (e.g., car-

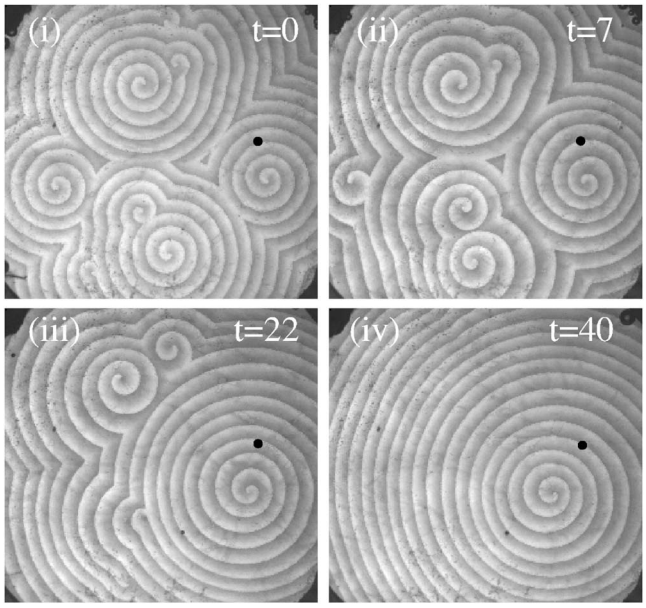

FIG. 1. A series of images of a spatially forced experiment; t (minutes) denotes time from the onset of imposing a light gradient. The location of minimum light intensity, denoted by (●), is closest to the rightmost spiral vortex; intensity increases radially from (●). Light affects the spiral vortex frequency; as intensity increases, frequency decreases. The spiral domain with highest frequency (rightmost) overtakes domains of lower frequency so that eventually only one spiral domain remains. The remaining spiral drifts to the left after (iv) (not shown). Image size 13.2 mm × 14.1 mm. Experimental chemical conditions given in Sec. II A.

*Electronic address: lsmolka@bucknell.edu
†Electronic address: alin@phy.duke.edu

diac tissue), thus understanding the effect of inhomogeneities on the dynamics of spirals is important.

In an analytical study examining the effect of slowly varying spatial inhomogeneities on spiral waves, Hendrey *et al.* [18,19] relate the grain boundary motion to the frequency and wave number of the spirals using the complex Ginzburg Landau equation. We test their theoretical results quantitatively in experiments using the BZ reaction. The experimental results and theoretical predictions show reasonable quantitative agreement.

A. Theoretical background

An analytical study of the effect of weak spatial inhomogeneities has been made using the 2D complex Ginzburg-Landau (CGL) equation

$$\partial_t A = \mu A - (1 + i\alpha)|A|^2 A + (1 + i\beta)\nabla^2 A, \tag{1}$$

where the terms on the right represent weak growth, nonlinearity and spatial coupling of the amplitude, respectively. The spatial inhomogeneity is imposed through the growth rate, $\mu = \mu(x,y)$ [18,19]. Simulations of Eq. (1) reveal that an inhomogeneity causes spirals at different positions to have different frequencies [18,19]. Furthermore, the frequency difference between neighboring spiral domains cause the grain boundary to move. If the spiral vortices are far from the grain boundary, then the boundary moves with a velocity

$$v_{\text{boundary}} = \frac{\omega_1 - \omega_2}{k_1 + k_2}, \tag{2}$$

where ω_1, ω_2, k_1 and k_2 represent, respectively, the frequency and wave number normal to the grain boundary of the two spirals [23]. As the grain boundary moves, one spiral gains area while the other loses area. As the grain boundary approaches the "weaker" spiral vortex, the boundary and vortex interact; the boundary sweeps away the weaker spiral at the predicted speed

$$v_{\text{sweep}} = \left| \frac{\omega_D - \omega_L}{k_D} \right|, \tag{3}$$

where now we use the notation D and L to distinguish between the dominant and weaker spirals, respectively [18,19]. (We will provide criteria that identify the weaker and dominant spirals in our experiments.) As time evolves, all weaker spirals are swept away and the dominant spiral occupies nearly the entire space. In simulations of the CGL [18,19], if $\beta > \alpha (\beta < \alpha)$, then the higher (lower) frequency spiral grows while the lower (higher) frequency spiral shrinks. A spatial inhomogeneity also causes the spiral vortices to drift [8,14,18,19]. This drift occurs on a slower time scale than the motion of the grain boundaries [Eqs. (2) and (3)] [18,19]. In particular, the remaining spiral vortex in the domain approaches a fixed point as the drift speed approaches zero at very long times [18,19].

In several studies, the CGL equation has done a remarkable job modeling phenomena observed in the BZ reaction [24–26], yet no direct connection has thus far been made between the model's growth parameter μ and the reaction, though a method has been developed to experimentally determine the parameters α, β in a homogeneous system [27]. As a result, we are unable to experimentally impose the same spatial inhomogeneity used by Hendrey *et al.* Despite this, we are able to quantitatively test the relations between the grain boundary speed and the frequency and wave number of the spirals given by Eqs. (2) and (3) in the BZ reaction.

An example of the BZ reaction under spatially inhomogeneous conditions is shown in Fig. 1. At the beginning of an experiment a typical initial pattern of several spiral domains is allowed to develop under spatially homogeneous conditions. We then apply light to the membrane for the next 4 hours, with a light intensity that increases radially away from the closed circle (●). As time evolves the highest frequency (rightmost) spiral becomes larger and larger so that eventually the other spiral vortices are swept off the membrane [(ii)–(iv)]. It is well known in spatially extended systems with multiple spirals of different frequency that the highest frequency spiral is the asymptotically stable pattern [6,21]. After frame (iv), the remaining spiral continues to drift without reaching a fixed point.

The paper is organized as follows. Section II details the experimental methods and data analysis. Section III contains the experimental results detailing the qualitative and quantitative experimental observations, along with comparisons to the predictions by Hendrey *et al.* [18,19]. Conclusions are provided in Sec. IV.

II. EXPERIMENTAL METHODS

A. Experimental setup

We use the same BZ experimental setup as in [22,28–30]. The reaction takes place in a thin porous Vycor glass membrane sandwiched between two chemical reservoirs. The glass membrane is 0.4 mm thick and 22 mm in diameter. Reagents diffuse homogeneously from the continuously stirred reservoirs into the glass through its two faces. The pattern wavelength is $\geqslant$0.5 mm while the membrane is 0.4 mm thick, so the pattern is quasi-two-dimensional. Each 8.3 mL volume reservoir is continuously refreshed at a flow rate of 20 mL/h. The two reservoirs (A and B) contain 0.8 M sulfuric acid (A,B); 0.184 M potassium bromate (A); 0.001 M tris(2,2 '-bipyridyl)dichlororuthenium(II) hexahydrate (A); 0.264 M potassium bromate (B); 0.22 M malonic acid (B); and 0.2 M sodium bromide (B). Under these conditions the reaction is oscillatory and we observe rotating spiral waves of Ru(II) concentration in the membrane.

The spiral waves are imaged by passing spatially homogeneous low-intensity light through the membrane and measuring the relative intensity of the transmitted light using a CCD camera (COHU), bandpass filtered at 451 nm. Regions of the glass membrane that contain high Ru(II) concentration absorb more light at 451 nm; regions of low intensity have a higher concentration of Ru(II). Video images are acquired at 2 s/frame.

B. Initial conditions

Tracking the simultaneous movement of multiple spiral domains, as shown in Fig. 1, can be complicated. In order to

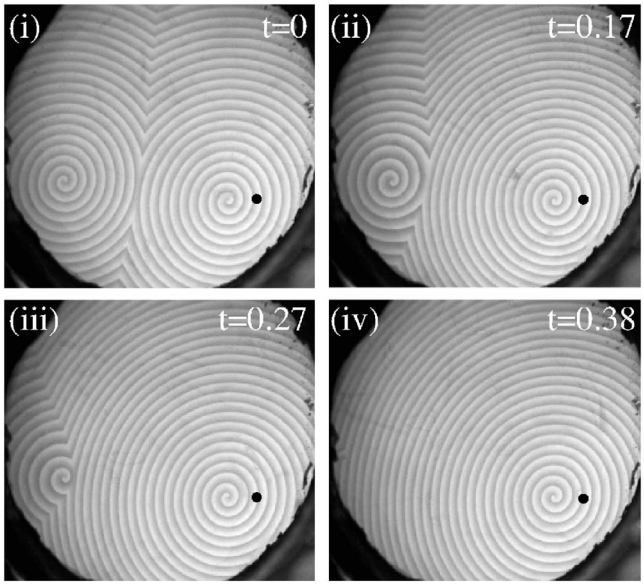

FIG. 2. Two spiral domains separated by a grain boundary; t (hours) denotes time from the onset of the light gradient. The light intensity increases radially from (●). The frequency of the spiral pattern under homogeneous conditions is $\omega=0.0906\ s^{-1}$. Once the light gradient is applied, the pattern frequency is set by the individual spiral vortices; the right (left) domain frequency is $\omega=0.0886\ s^{-1}(0.0728\ s^{-1})$. The grain boundary sweeps to the left as the higher (lower) frequency domain gains (loses) area in time. The left spiral vortex interacts with the grain boundary once the boundary is within a wavelength of the vortex (iii). The grain boundary sweeps the spiral vortex off the membrane shortly thereafter [between (iii) and (iv)]. Image size 14.9 mm × 19.4 mm. Experimental chemical conditions given in Sec. II A.

simplify the comparison between experimental data and theoretical predictions for the grain boundary speeds given by Eqs. (2) and (3) [18,19], we establish simple initial conditions: in all of our experiments, two spiral vortices are initially arranged on the membrane [e.g., see Fig. 2(i)]. The advantage of a two spiral setup is only one grain boundary must be tracked.

C. Spatial inhomogeneity

We project a time independent spatial gradient of light on the membrane. The ruthenium catalyst of the BZ chemical reaction is light sensitive [10,22,31]. For our experimental conditions, the spiral frequency decreases with increasing light intensity as shown in Fig. 3. Given the symmetry of the spiral patterns, we use an axisymmetric spatial gradient, with the light intensity increasing radially from $r=0$. In the experiments, the minimum of the light intensity was placed at various locations relative to the two spiral vortices, including closer to one of the spiral vortices (as in Fig. 2) and equidistant from the spiral vortices.

The light gradient is applied using a commercial video projector (Sanyo PLC-750M) with a condensing lens. The video projector is computer controlled using a video card with a refresh rate of at least 0.1 s.

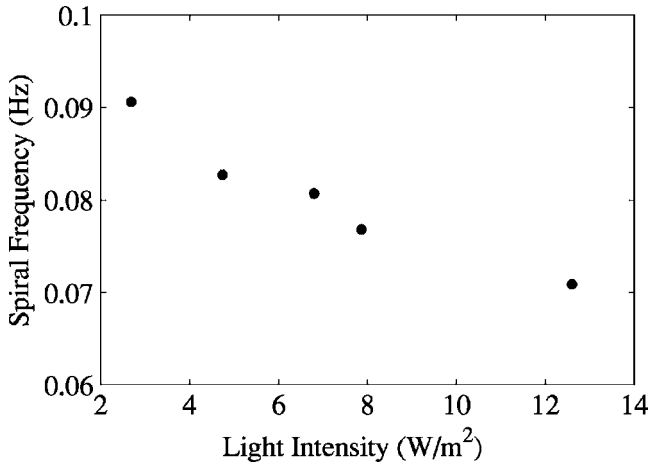

FIG. 3. Spiral frequency as a function of steady, homogeneous light intensity. Experimental chemical conditions given in Sec. II A.

D. Experimental procedure

In each run, the experiment was setup and allowed to equilibrate for at least one hour under spatially homogeneous conditions. Typically during this stage several spiral domains developed on the membrane [e.g., see Fig. 1(i)]. Using the reaction's sensitivity to light, all undesired spiral vortices were annihilated by projecting light in a small neighborhood surrounding their core (light decreases spiral frequency causing neighboring, higher frequency spiral domains to overtake the lower frequency spiral), leaving only two spiral domains on the membrane. The resulting two-spiral pattern, allowed to equilibrate for at least half an hour in homogeneous conditions, was found to have a constant frequency in space and time before a light gradient was projected across the entire membrane. In addition, the grain boundary between the two spirals did not move during this time period. Then, over the next four hours a light gradient was applied to the entire membrane and the response of the spiral pattern was tracked.

E. Data analysis

Video images in the experiment are $240\times320(\text{pixels})^2$ in size. To compare the motion of the grain boundary to the predictions given by Eqs. (2) and (3), we measured the location of the boundary, and the frequency and wave number of each spiral over time. The location of the grain boundary at a given time was chosen to be the intersection of the boundary with a line connecting the two spiral vortices (±1 pixel). The spiral frequency $\omega_{1,2}$ was determined using a temporal fast Fourier transform over a rectangular area surrounding spiral vortex 1 or vortex 2, respectively. The frequency was determined by taking the average of the power spectrum of the pixels in the rectangle and is accurate to within $\pm0.002\ s^{-1}$. The wave number $k_{1,2}$ equals $2\pi/\lambda_{1,2}$, where $\lambda_{1,2}$ is the wavelength of the last full wave in the spiral domain of spiral 1 or 2 before reaching the grain boundary. The actual speed of the grain boundary was obtained by taking the ratio of the boundary displacement over time, representing an average speed. The resolution of measured quantities were calculated following [32].

III. EXPERIMENTAL RESULTS

In all of our experiments, the spiral patterns were stable before the light gradient was applied. That is, stationary spiral vortices persisted in time and no noticeable movement was observed in the grain boundaries separating spiral domains for periods up to 1–2 hours. In addition, the frequency of the spiral pattern was constant in space and time (within the resolution of our measurements). For example, the frequency of the data shown in Fig. 2, measured prior to projecting the light gradient, is $\omega=0.0906\ \mathrm{s}^{-1}$ across the *entire* membrane.

We find that each spiral vortex acts as a pacemaker, setting the frequency for its entire domain; the frequency of an entire spiral domain is equal to the vortex frequency set by the light intensity at the vortex position. This observation is analogous to observations made in a series of single spiral experiments by Belmonte and Flesselles [12]. In their experiments the entire spiral domain adjusted to a different uniform period and pitch when laser light was directed at the spiral core, with the period and pitch increasing functions of light intensity [12]. Once the light source was removed, the spiral period and pitch relaxed back to their lower, unforced values [12].

In the experiment shown in Fig. 2 the minimum light intensity is centered closer to the right spiral so that once the light gradient is applied, the frequency of the right spiral domain ($\omega_1=0.0886\ \mathrm{s}^{-1}$) is greater than the left spiral domain ($\omega_2=0.0728\ \mathrm{s}^{-1}$). This variation in the spiral domain frequencies cause the grain boundary to move with the right domain increasing in area while the left domain decreases in area [compare frames (i)–(iii)]. Hence, the dominant (weaker) spiral is the higher (lower) frequency spiral. The motion of the grain boundary between the spiral domains is relatively rapid; in less than 23 minutes the grain boundary sweeps the left spiral off the membrane.

Figure 4 shows measurements of the grain boundary speed compared to the predicted speeds given by Eqs. (2) and (3) for the experiment in Fig. 2. The measured boundary speed is an averaged quantity, and is represented by the open circles and horizontal dashed lines (which denote the interval over which the average was determined). Between $0 \leqslant t \leqslant 0.25$ h, the spirals are sufficiently far from the grain boundary so Eq. (2) applies. Over this time interval, the predicted speed Eq. (2) agrees well with the measured speed, see Fig. 4; the average measured and predicted grain boundary speeds are 13.6 and 15.7 mm/h (run 1 in Table I), respectively. Data from four other experiments are also shown in Table I. Like run 1, the conditions in run 5 are such that the minimum light intensity was placed closer to one of the spiral vortices, leading to a larger difference in the frequency of the two spiral vortices, and thus a larger average boundary speed. In runs 2 and 3 the minimum light intensity was centered nearly equidistant from each of the vortices, and in run 4 the spiral vortices were initially close to each other; as a consequence in each of these cases the frequency difference between the spiral domains was small resulting in a lower grain boundary speed. The theory correctly predicts this trend. Clearly Eq. (2) has a similar qualitative response, i.e., if $\omega_1-\omega_2$ is smaller then the predicted boundary speed will also be smaller.

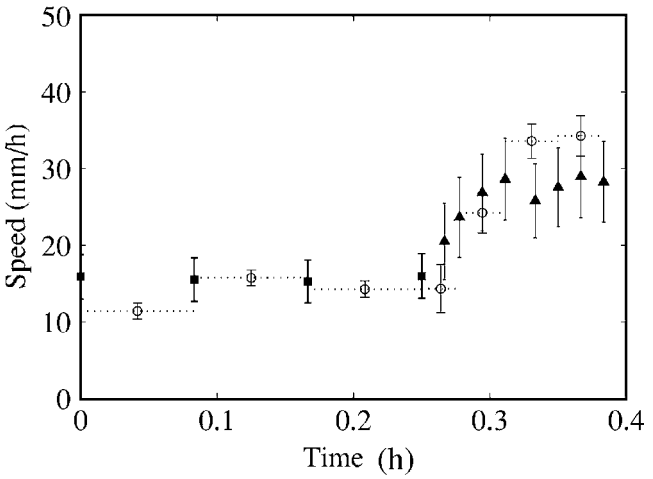

FIG. 4. Measurements of the grain boundary speed corresponding to the experiment shown in Fig. 2; symbols denote as follows: (○) measured grain boundary speed, (■) predicted grain boundary speed Eq. (2), and (▲) predicted sweep speed of the grain boundary Eq. (3). Time is referenced from the onset of the light gradient. Horizontal dashed lines indicate interval over which (○) is averaged. Vertical bars indicate resolution of quantities. Between $0 \leqslant t \leqslant 0.25$ h, the spirals are sufficiently far from the grain boundary so that Eq. (2) applies. Within the resolution bars, agreement between the average boundary speed and Eq. (2) is strong. For $t > 0.25$ h, the left spiral interacts with the grain boundary so Eq. (3) applies. Over this time interval, the average speed of the grain boundary (○) increases as predicted by Eq. (3).

When the grain boundary is within a wavelength of a spiral vortex, the vortex interacts with the boundary, and the corresponding boundary speed changes to Eq. (3) according to [18,19] (where D and L represent the higher and lower frequency spirals, respectively). In the experiment shown in Fig. 2, the left spiral vortex begins to interact with the grain boundary in frame (iii). In a relatively short time interval (less than 8 minutes), the grain boundary sweeps the left spiral vortex off the membrane so that only the right spiral domain remains [frame (iv)]. Figure 4 shows measurements of the grain boundary sweeping speed and of Eq. (3), taken between frames (iii) and (iv) in Fig. 2. The theory correctly

TABLE I. Average speeds (mm/h) from experimental data and theoretical predictions: v_{boundary} grain boundary speed; v_{sweep} sweeping speed of lower frequency spiral by the grain boundary; and v_{drift} drift speed of higher frequency spiral.

	v_{boundary}		v_{sweep}		v_{drift}
Run	Measured	$\frac{\omega_1-\omega_2}{k_1+k_2}$	Measured	$\lvert\frac{\omega_D-\omega_L}{k_D}\rvert$	Measured
1	13.6	15.7	29.0	26.4	0.6
2	4.5	4.7	10.7	9.1	1.4
3	1.9	2.4			1.5
4	3.2	5.0			0.9
5	7.5	6.5			2.3

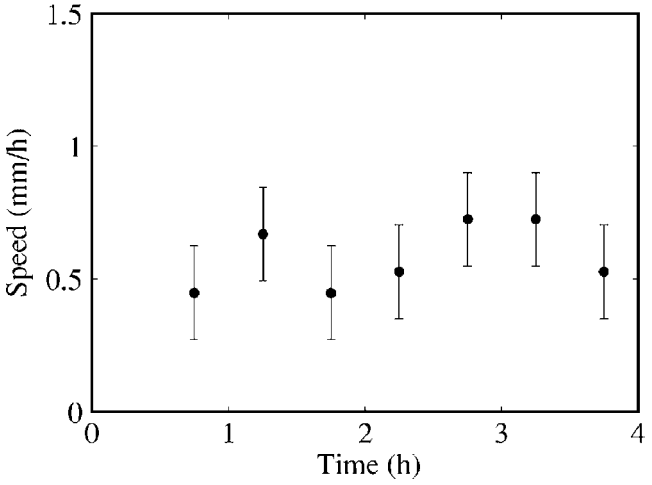

FIG. 5. The measured drift of the remaining spiral for the experiment shown in Fig. 2. Time is referenced from the onset of projecting the light gradient. The average drift speed (0.6 mm/h) is constant within the experimental resolution, and is two orders of magnitude lower than the grain boundary speed shown in Fig. 4.

predicts the trend of increasing speed within the resolution bars of Fig. 4. The average measured and predicted sweep speeds over this time interval are 29.0 and 26.4 mm/h for run 1 (Table I), respectively. We observed similar behavior in run 2, with the average sweep speeds from the experiment and theory reported in Table I. In runs 3, 4 and 5 the lower frequency spiral did not strongly interact with the grain boundary, and as a result the sweep speed could not be measured. For instance, in run 5 the lower frequency spiral was pushed off the membrane while the grain boundary was still far from this vortex.

We observe in all of our experiments that the remaining (highest frequency) spiral vortex drifts away from the optimal location in the domain where the light intensity is a minimum. Similar behavior was observed in simulations of the CGL equation by Hendrey *et al.* where the spiral vortex drifts away from the position with the highest frequency. Since a direct connection between the CGL parameters μ, α, β and the BZ reaction is not known, we are unable to compare the drift speed of the vortex in the experiments to the prediction (Eq. (17) in [19]). In the experiments the drift speed ranged between a factor to two orders of magnitude less than the grain boundary speed (see Table I). An example of the drift speed is shown in Fig. 5 where the data is taken after Fig. 2(iv) (run 1). Within the resolution bars the drift speed is constant at 0.6 mm/h, which is two orders of magnitude lower than the grain boundary speeds (Fig. 4). We note that in all the experiments, the drift speed of the highest frequency spiral is lower than the speed of the grain boundary (and sweep speed where applicable), confirming the assertion by Hendrey *et al.* that these two activities occur on different time scales.

In all of the experiments, we find the spiral vortex does not attain a fixed point with the drift speed approaching zero contradicting the numerical results of Hendrey *et al.* [18,19]. There are three plausible explanations for this difference in results: the spatial inhomogeneity in our experiments may be stronger than that used by Hendrey *et al.*; the experiments after four hours may not have attained their long term asymptotic state as in the numerical simulations (e.g., in run 1 the spiral vortex has drifted ~ 2 mm which may be far from the distance necessary to reach a fixed point); or the experimental conditions are far from the Hopf bifurcation which is where the CGL equations are valid.

IV. CONCLUSIONS

We find the frequency of oscillations is nearly constant within a spiral domain and is set by the spiral vortex consistent with the numerical findings of Hendrey *et al.* [18,19]. In all of the experiments, we observe that the highest frequency spiral domain grows causing the lower frequency spiral domains to shrink so that at long times only the highest frequency spiral remains. According to the theoretical results of Hendrey *et al.* [18,19], this means that $\beta > \alpha$ in our experimental BZ system. To our knowledge, this is the first time a connection has been made between the parameters β and α in the inhomogeneous BZ system and the CGL model.

We find predictions of the grain boundary and sweep speeds Eqs. (2) and (3) [18,19] agree well with experimental data in the BZ system; this confirms the motion of the grain boundary is due to the interaction of neighboring spiral domains and depends simply on the frequency and wave number of the spiral pattern. At long times, the remaining spiral drifts away from the optimal position in the domain at a speed slower than the grain boundary and sweep speeds. According to [18,19] this drift should be linearly related to the gradient of the inhomogeneity, however, it is unclear how to relate this prediction with the experimental conditions in the BZ system. Finally, we observe that in all of the experiments the remaining spiral vortex does not converge to a fixed point as observed in the numerical simulations of the CGL equations. There are three plausible explanations for this difference: the spatial inhomogeneity in the experiments may be stronger than that used in the simulations; the experiments may not have attained their long term asymptotic state; or our experiments are performed far from the Hopf bifurcation which is where the CGL equations are valid. Several strong qualitative and quantitative comparisons between the CGL predictions and experimental results from the BZ chemical reaction-diffusion system have been identified in this study.

ACKNOWLEDGMENTS

The authors wish to thank Karl Martinez and Edward Ott for many helpful discussions related to the experiment. L.B.S. acknowledges the support of the National Science Foundation while at Duke University (DMS-9983320). A.L.L. and B.M. acknowledge the support of the National Science Foundation (DMR-0348910).

[1] F. X. Witkowski, L. J. Leon, P. A. Penkoske, W. R. Giles, M. L. Spano, W. L. Ditto, and A. Winfree, Nature (London) **392**, 78 (1998).
[2] G. Bub, A. Shrier, and L. Glass, Phys. Rev. Lett. **88**, 058101 (2002).
[3] K. J. Lee, E. C. Cox, and R. E. Goldstein, Phys. Rev. Lett. **76**, 1174 (1996).
[4] N. Nishiyama, Phys. Rev. E **57**, 4622 (1998).
[5] S. Jakubith, H. H. Rotermund, W. Engel, A. von Oertzen, and G. Ertl, Phys. Rev. Lett. **65**, 3013 (1990).
[6] A. T. Winfree, Science **175**, 634 (1972).
[7] P. S. Hagan, SIAM J. Appl. Math. **42**, 762 (1982).
[8] R. R. Aliev and A. B. Rovinsky, J. Phys. Chem. **96**, 732 (1992).
[9] A. Karma, Phys. Rev. Lett. **71**, 1103 (1993).
[10] V. Petrov, Q. Ouyang, G. Li, and H. L. Swinney, J. Phys. Chem. **100**, 18992 (1996).
[11] T. Bohr, G. Huber, and E. Ott, Physica D **106**, 95 (1997).
[12] A. Belmonte and J.-M. Flesselles, Phys. Rev. Lett. **77**, 1174 (1996).
[13] I. V. Biktasheva, Y. E. Elkin, and V. N. Biktashev, Phys. Rev. E **57**, 2656 (1998).
[14] I. V. Biktasheva, Phys. Rev. E **62**, 8800 (2000).
[15] F. Xie, Z. Qu, J. N. Weiss, and A. Garfinkel, Phys. Rev. E **63**, 031905 (2001).
[16] M. Vinson, Physica D **116**, 313 (1998).
[17] C. X. Zhang, H. M. Liao, L. Q. Zhou, and Q. Ouyang, J. Phys. Chem. B **108**, 16990 (2004).
[18] M. Hendrey, E. Ott, and T. M. Antonsen, Jr., Phys. Rev. Lett. **82**, 859 (1999).
[19] M. Hendrey, E. Ott, and T. M. Antonsen, Jr., Phys. Rev. E **61**, 4943 (2000).
[20] J. Davidsen, L. Glass, and R. Kapral, Phys. Rev. E **70**, 056203 (2004).
[21] V. I. Krinsky and K. I. Agladze, Physica D **8**, 50 (1983).
[22] K. Martinez, A. L. Lin, R. Kharrazian, X. Sailer, and H. L. Swinney, Physica D **168–169**, 1 (2002).
[23] K. Nam, E. Ott, M. Gabbay, and P. N. Guzdar, Physica D **118**, 69 (1998).
[24] A. L. Lin, A. Hagberg, A. Ardelea, M. Bertram, H. L. Swinney, and E. Meron, Phys. Rev. E **62**, 3790 (2000).
[25] A. Yochelis, A. Hagberg, E. Meron, A. L. Lin, and H. L. Swinney, SIAM J. Appl. Dyn. Syst. **1**, 236 (2002).
[26] B. Marts, A. Hagberg, E. Meron, and A. L. Lin, Phys. Rev. Lett., **93**, 108305 (2004).
[27] F. Hynne and P. Graae Sørensen, Phys. Rev. E **48**, 4106 (1993).
[28] V. Petrov, Q. Ouyang, and H. L. Swinney, Nature (London) **388**, 655 (1997).
[29] A. L. Lin, M. Bertram, K. Martinez, H. L. Swinney, A. Ardelea, and G. F. Carey, Phys. Rev. Lett. **84**, 4240 (2000).
[30] B. Marts, K. Martinez, and A. L. Lin, Phys. Rev. E **70**, 056223 (2004).
[31] S. Kadar, T. Amemiya, and K. Showalter, J. Phys. Chem. A **101**, 8200 (1997).
[32] J. R. Taylor, *An Introduction to Error Analysis*, 2nd ed. (University Science Books, Sausalito, CA, 1997).